Supporting Information

Phosphorous complexes of a triply-fused [24]pentaphyrin

Tomohiro Higashino, and Atsuhiro Osuka*

Department of Chemistry, Graduate School of Science, Kyoto University, Sakyo-ku, Kyoto 606-8502, Japan

E-mail: osuka@kuchem.kyoto-u.ac.jp

Contents

1. Experimental Section

Instrumentation and Materials.

Commercially available solvents and reagents were used without further purification unless otherwise mentioned. Dry CH_2Cl_2 was obtained by refluxing and distillation over CaH_2. Dry toluene was obtained by refluxing and distillation over CaH_2. Silica-gel column chromatography was performed on Wakogel C-300 or C-400. Alumina column chromatography was performed on Sumitomo Active alumina. UV/Vis absorption spectra were recorded with a Shimadzu UV-3100PC spectrometer. ^{1}H, ^{19}F, ^{31}P and ^{11}B NMR spectra were recorded with a JEOL ECA-600 spectrometer (operating at 600.17 MHz for ^{1}H, 150.91 MHz for ^{13}C, 564.73 MHz for ^{19}F, 242.95 MHz for ^{31}P, and 192.56 MHz for ^{11}B) by using the residual solvent as the internal reference for ^{1}H ($CDCl_3$: $\delta = 7.26$ ppm), the residual solvent as the internal reference for ^{13}C ($CDCl_3$: $\delta = 77.16$ ppm, CD_2Cl_2: $\delta = 53.84$ ppm), hexafluorobenzene as the external reference for ^{19}F ($\delta = -162.9$ ppm), 85% phosphoric acid as the external reference for ^{31}P ($\delta = 0.00$ ppm), and $BF_3{\cdot}Et_2O$ as the external reference for ^{11}B ($\delta = 0.00$ ppm). NMR signals were assigned from the ^{1}H–^{1}H COSY, ^{19}F–^{19}F COSY, ^{1}H–^{31}P HMBC spectra, and the comparison with the spectra in the presence of D_2O (signals assigned for NH protons disappear in the presence of D_2O). Mass spectra were recorded with a BRUKER microTOF LC by using the ESI-TOF method in the positive ion mode and in the negative ion mode in an acetonitrile solution. Single-crystal X-ray diffraction analysis data for compound **2**, **3**, and **4** were collected at –180 °C with a Rigaku R-AXIS RAPID II diffraction by using graphite monochromated Cu-K_α radiation (λ = 1.54187 Å). The structures were solved by direct method (SHELXS-97). Redox potentials were measured by cyclic voltammetry method on an ALS electrochemical analyzer model 660.

2. Synthesis

meso-Pentakis(pentafluorophenyl)-substituted *N*-fused [24]pentaphyrin(1.1.1.1.1) (1):

For **1**, the synthetic details were previously described.[S1]

Phosphine oxide complex of *meso*-pentakis(pentafluorophenyl)-substituted *N*-fused [24]pentaphyrin(1.1.1.1.1) (2):

A dry flask containing **1** (31.0 mg, 25 μmol) was filled with N_2, to which were added toluene (25 mL), $POCl_3$ (0.23 mL, 2.5 mmol) and triethylamine (0.70 mL, 5.0 mmol). The reaction mixture was stirred for 12 h under N_2 atmosphere at 120 ˚C. Then, the reaction was quenched by the addition of

water, and the product was extracted with ethyl acetate (3 × 25 mL). The combined organic layer was washed with water and dried over Na_2SO_4 and the solvent was removed. The crude product was purified by silica gel column chromatography using CH_2Cl_2 to give an orange fraction. Recrystallization from CH_2Cl_2 and *n*-hexane gave brown solid of **2** (20.7 mg, 16.7 μmol, 66%). Single crystals suitable for X-ray crystallographic analysis were obtained by vapor diffusion of hexane into chlorobenzene solution of **2**.

2: ^{1}H NMR (600.17 MHz, $CDCl_3$, 25 ˚C): δ = 6.35 (d, J = 4.8 Hz, 1H, β_D), 6.05 (d, J = 4.8 Hz, 1H, β_D), 4.59 (t, J = 3.4 Hz, 1H, β_A), 4.43 (quintet, J = 4.8 Hz, 1H, β_A), and 4.34 (d, J = 2.0 Hz, 2H, β_B) ppm; ^{13}C NMR (150.91 MHz, CD_2Cl_2, 25 ˚C): δ = 150.5, 145.6, 145.0, 144.9, 144.7, 144.5, 144.4, 144.2, 143.2, 143.0, 142.8, 142.3, 142.0, 141.9, 141.5, 141.1, 141.0, 140.2, 140.1, 139.7, 139.5, 139.1, 138.3, 138.2, 138.1, 137.9, 137.8, 137.5, 137.3, 134.2, 139.8, 129.5, 129.3, 129.2, 127.0, 126.9, 125.1, 124.4, 123.3, 123.1, 123.0, 122.8, 122.0, 121.9, 119.5, 116.7, 113.1, 110.4, 106.4, 106.0, 104.8, 102.9, 100.3, 99.6, and 96.2 ppm; ^{19}F NMR (564.73 MHz, $CDCl_3$, 25 °C): δ = –133.46 (d, J = 24.2 Hz, 1F, *ortho*-F), –134.25 (m, 1F), –135.60 (d, J = 24.2 Hz, 1F, *ortho*-F), –136.43 (d, J = 24.2 Hz, 1F, *ortho*-F), –136.55 (d, J = 24.2 Hz, 1F, *ortho*-F), –137.22 (d, J = 20.7 Hz, 1F, *ortho*-F), –137.30 (d, J = 20.7 Hz, 1F, *ortho*-F), –137.46 (d, J = 17.3 Hz, 1F, *ortho*-F), –137.88 (d, J = 24.2 Hz, 1F, *ortho*-F), –150.08 (t, J = 20.7 Hz, 1F, *para*-F), –151.17 (t, J = 20.7 Hz, 1F, *para*-F), –152.12 (t, J = 20.7 Hz, 1F, *para*-F), –153.82 (t, J = 20.7 Hz, 1F, *para*-F), –154.51 (t, J = 20.7 Hz, 1F), –158.97 (td, J = 24.2 Hz, J = 10.4 Hz, 1F, *meta*-F), –159.68 (td, J = 20.7 Hz, J = 6.9 Hz, 1F, *meta*-F), –159.98 (td, J = 20.7 Hz, J = 6.9 Hz, 1F, *meta*-F), –160.48 (td, J = 20.7 Hz, J = 10.4 Hz, 1F, *meta*-F), –160.65 (t, J = 17.3 Hz, 1F), –161.90 (td, J = 20.7 Hz, J = 6.9 Hz, 1F, *meta*-F), –162.14 (m, 2F, *meta*-F), –162.92 (t, J = 20.7 Hz, 1F, *meta*-F), and –163.82 (t, J = 20.7 Hz, 1F) ppm; ^{31}P NMR (242.95 MHz, $CDCl_3$, 25 °C): δ = 7.12 (s) ppm. UV/vis: $\lambda_{max}(CH_2Cl_2)$/nm 319 (ε/dm^3 mol^{-1} cm^{-1} 45000), 398 (47000), 473 (25000), 561 (10000), 696 (2000) and 770 (1600). HRMS (ESI-TOF, negative) calcd. for $C_{55}H_6F_{24}N_5OPCl$ $[M+Cl]^-$ 1273.9621; found 1273.9612.

Phosphine sulfide complex of *meso*-pentakis(pentafluorophenyl)-substituted *N*-fused [24]pentaphyrin(1.1.1.1.1) (3):

A dry flask containing **2** (11.5 mg, 9.3 μmol) and Lawesson's Reagent (7.8 mg, 19 μmol) was filled with N_2, to which were added toluene (25 mL). The reaction mixture was refluxed for 1 h under N_2 atmosphere, and then cooled down. After evaporation of the solvent, the residue was separated by silica gel column chromatography using a 1:1 mixture of CH_2Cl_2 and *n*-hexane to give an orange fraction. Recrystallization from CH_2Cl_2 and *n*-hexane gave brown solid of **3** (9.7 mg, 7.8 μmol, 84%). Single crystals suitable for X-ray crystallographic analysis were obtained by vapor diffusion of

heptane into toluene solution of **3**.

3: ^{1}H NMR (600.17 MHz, $CDCl_3$, 25 ˚C): δ = 6.18 (d, J = 4.8 Hz, 1H, β_D), 5.88 (d, J = 4.8 Hz, 1H, β_D), 4.36 (s, 1H, β_A), 4.26 (quintet, J = 4.8 Hz, 1H, β_A), 4.16 (d, J = 5.5 Hz, 1H, β_B), and 4.13 (d, J = 5.5 Hz, 1H, β_B) ppm; ^{13}C NMR (150.91 MHz, $CDCl_3$, 25 ˚C): δ = 165.0, 164.9, 155.3, 153.3, 153.1, 150.2, 145.2, 144.6, 144.4, 144.3, 144.2, 144.1, 143.8, 142.5, 142.0, 141.6, 141.4, 140.8, 140.1, 139.6, 139.5, 137.8, 137.7, 137.4, 137.3, 137.2, 137.0, 136.8, 133.8, 133.6, 131.5, 131.4, 129.6, 129.3, 129.2, 127.6, 127.5, 126.3, 125.3, 125.2, 124.3, 123.5, 122.9, 122.7, 122.3, 121,7, 121.6, 115.9, 109.8, 105.9, 105.6, 104.3, 103.3, 99.9, and 99.7 ppm; ^{19}F NMR (564.73 MHz, $CDCl_3$, 25 °C): δ = –133.27 (d, J = 24.2 Hz, 1F, *ortho*-F), –134.11 (m, 1F), –135.70 (d, J = 24.2 Hz, 1F, *ortho*-F), –136.24 (t, J = 24.2 Hz, 2F, *ortho*-F), –137.35 (d, J = 24.2 Hz, 1F, *ortho*-F), –137.46 (d, J = 20.7 Hz, 1F, *ortho*-F), –137.72 (d, J = 20.7 Hz, 2F, *ortho*-F), –150.34 (t, J = 20.7 Hz, 1F, *para*-F), –151.45 (t, J = 20.7 Hz, 1F, *para*-F), –152.32 (t, J = 20.7 Hz, 1F, *para*-F), –154.11 (t, J = 20.7 Hz, 1F, *para*-F), –155.04 (t, J = 20.7 Hz, 1F), –159.20 (td, J = 24.2 Hz, J = 10.3 Hz, 1F, *meta*-F), –159.78 (td, J = 20.7 Hz, J = 10.3 Hz, 1F, *meta*-F), –160.08 (td, J = 20.7 Hz, J = 6.9 Hz, 1F, *meta*-F), –160.60 (td, J = 24.2 Hz, J = 10.3 Hz, 1F, *meta*-F), –160.71 (t, J = 17.3 Hz, 1F), –162.05 (td, J = 24.7 Hz, J = 6.9 Hz, 1F, *meta*-F), –162.25 (m, 2F, *meta*-F), –163.08 (t, J = 20.7 Hz, 1F, *meta*-F), and –164.06 (t, J = 20.7 Hz, 1F) ppm; ^{31}P NMR (242.95 MHz, $CDCl_3$, 25 °C): δ = 58.55 (s) ppm. UV/vis: $\lambda_{max}(CH_2Cl_2)$/nm 318 (ε/dm^3 mol^{-1} cm^{-1} 51000), 403 (55000), 477 (33000), 581 (13000), 707 (2700) and 784 (2500) nm. HRMS (ESI-TOF, negative) calcd. for $C_{55}H_6F_{24}N_5SPCl$ $[M+Cl]^-$ 1289.9392; found 1289.9379.

Phosphine-borane complex of *meso*-pentakis(pentafluorophenyl)-substituted *N*-fused [24]pentaphyrin(1.1.1.1.1) (4):

A dry flask containing **2** (12.3 mg, 10 μmol) was filled with N_2, to which were added CH_2Cl_2 (10 mL) and BH_3·SMe_2 (19 μL). The reaction mixture was stirred for 24 h under N_2 atmosphere. After evaporation of the solvent, the residue was separated by silica gel column chromatography using a 1:1 mixture of CH_2Cl_2 and *n*-hexane to give an orange fraction. Recrystallization from CH_2Cl_2 and *n*-hexane gave brown solid of **4** (6.7 mg, 5.4 μmol, 54%). Single crystals suitable for X-ray crystallographic analysis were obtained by vapor diffusion of hexane into toluene solution of **4**.

4: ^{1}H NMR (600.17 MHz, $CDCl_3$, 25 ˚C): δ = 7.22 (d, J = 4.2 Hz, 1H, β_D), 6.96 (d, J = 4.2 Hz, 1H, β_D), 6.33 (quintet, J = 4.8 Hz, 1H, β_A), 5.57 (d, J = 3.5 Hz, 1H, β_A), 2.65 (m, 1H, β_B), 2.53 (m, 1H, β_B), 2.37 (m, 1H, β_B), 2.28 (br, 3H, BH_3), and 2.18 (m, 1H, β_B) ppm; ^{13}C NMR (150.91 MHz, $CDCl_3$, 25 ˚C): δ = 159.2, 159.1, 153.3, 153.2, 151.2, 145.7, 145.2, 145.0, 144.9, 144.5, 142.6, 142.2, 141.9, 141.7, 141,4, 141.2, 141.1, 139.9, 138.2, 138.1, 138.0, 137.9, 137.7, 137.6, 137.4, 136.9, 134.7, 134.4, 134.2, 134.1, 134.0, 131.9,

127.5, 127.4, 127.1, 127.0, 123.6, 122.0, 121.9, 121.2, 119.2, 117.2, 117.0, 112.7, 111.4, 108.8, 108.5, 106.1, 105.7, 105.6, 101.0, 99.2, 96.8, 27.0, and 24.5 ppm; ^{19}F NMR (564.73 MHz, $CDCl_3$, 25 °C): δ = –133.44 (d, J = 24.2 Hz, 1F, *ortho*-F), –133.90 (m, 1F), –135.88 (d, J = 24.2 Hz, 1F, *ortho*-F), –136.89 (d, J = 24.2 Hz, 1F, *ortho*-F), –137.17 (d, J = 20.7 Hz, 1F, *ortho*-F), –137.44 (d, J = 24.2 Hz, 1F, *ortho*-F), –137.78 (t, J = 24.2 Hz, 2F, *ortho*-F), –137.86 (d, J = 20.7 Hz, 1F, *ortho*-F), –150.41 (t, J = 20.7 Hz, 1F, *para*-F), –151.94 (t, J = 20.7 Hz, 1F, *para*-F), –152.32 (t, J = 20.7 Hz, 1F, *para*-F), –153.94 (t, J = 20.7 Hz, 1F, *para*-F), –154.38 (t, J = 20.7 Hz, 1F), –159.54 (td, J = 24.2 Hz, J = 6.9 Hz, 1F, *meta*-F), –160.02 (m, 2F), –160.32 (td, J = 20.7 Hz, J = 6.9 Hz, 1F, *meta*-F), –160.55 (td, J = 24.2 Hz, J = 6.9 Hz, 1F, *meta*-F), –161.85 (td, J = 20.7 Hz, J = 6.9 Hz, 1F, *meta*-F), –162.07 (td, J = 24.2 Hz, J = 6.9 Hz, 1F, *meta*-F), –162.36 (t, J = 20.7 Hz, 1F, *meta*-F), –163.29(t, J = 20.7 Hz, 1F, *meta*-F), and –163.68 (t, J = 20.7 Hz, 1F) ppm; ^{31}P NMR (242.95 MHz, $CDCl_3$, 25 °C): δ = 119.22 (br) ppm; ^{11}B NMR (192.56 MHz, $CDCl_3$, 25 °C): δ = –32 ~ –33 (br) ppm. UV / vis: $\lambda_{max}(CH_2Cl_2)$ / nm 355 (sh) (ε / dm^3 mol^{-1} cm^{-1} 44000), 393 (54000), 479 (20000), 571 (8200), 645 (3000) and 865 (2800) nm. HRMS (ESI-TOF, negative) calcd. for $C_{55}H_{10}F_{24}N_5PB$ [M–H]$^-$ 1238.0398; found 1238.0370.

Phosphine oxide complex of chlorin-type *meso*-pentakis(pentafluorophenyl)-substituted *N*-fused [24]pentaphyrin(1.1.1.1.1) (5):

A dry Schlenk flask containing **4** (12.4 mg, 10 μmol) was filled with N_2, to which were added freshly distilled CH_2Cl_2 (2 mL) and freshly distilled triethylamine (28 μL, 200 μmol). The reaction mixture was stirred for 12 h under N_2 atmosphere. The reaction mixture was passed through a short silica gel column followed by evaporation of the solvent. The residue was separated by silica gel column chromatography using CH_2Cl_2 to give an orange fraction. Recrystallization from CH_2Cl_2 and *n*-hexane gave brown solid of **5** (3.8 mg, 3.1 μmol, 31%). Single crystals suitable for X-ray crystallographic analysis were obtained by vapor diffusion of water into acetonitrile / tetrachloromethane solution of **5**.

5: ^{1}H NMR (600.17 MHz, $CDCl_3$, 25 ˚C): δ = 7.39 (d, J = 4.8 Hz, 1H, β_D), 7.12 (d, J = 4.8 Hz, 1H, β_D), 6.42 (quintet, J = 4.8 Hz, 1H, β_A), 5.74 (s, 1H, β_A), 2.88 (m, 1H, β_B), 2.73 (m, 1H, β_B), 2.56 (m, 1H, β_B), and 2.38 (m, 1H, β_B) ppm; ^{13}C NMR (150.91 MHz, $CDCl_3$, 25 °C): δ = 159.2, 159.1, 153.3, 153.2, 151.2, 145.7, 145.3, 145.0, 144.9, 144.5, 142.6, 142.2, 141.9, 141.7, 141.4, 141.2, 141.1, 139.9, 138.2, 138.1, 138.0, 137.9, 137.7, 137.6, 137.5, 137.4, 136.9, 134.7, 134.4, 134.2, 134.1, 134.0, 131.9, 127.5, 127.4, 127.0, 123.6, 122.0, 121.9, 121.2, 119.2, 117.2, 117.0, 112.7, 111.4, 108.8, 108.5, 106.1, 105.7, 105.6, 101.0, 99.2, 96.8, 26.9, and 24.5 ppm; ^{19}F NMR (564.73 MHz, $CDCl_3$, 25 °C): δ = –133.50 (d, J = 24.2 Hz, 1F, *ortho*-F), –134.30 (m, 1F), –136.00 (d, J = 17.3 Hz, 1F, *ortho*-F), –136.89 (t, J = 24.2 Hz, 2F, *ortho*-F), –137.28 (d, J

= 20.7 Hz, 1F, *ortho*-F), –137.32 (d, *J* = 24.2 Hz, 1F, *ortho*-F), –137.72 (d, *J* = 20.7 Hz, 1F, *ortho*-F), –137.99 (d, *J* = 24.2 Hz, 1F, *ortho*-F), –150.25 (t, *J* = 20.7 Hz, 1F, *para*-F), –151.65 (t, *J* = 20.7 Hz, 1F, *para*-F), –152.11 (t, *J* = 20.7 Hz, 1F, *para*-F), –153.62 (t, *J* = 20.7 Hz, 1F, *para*-F), –153.98 (t, *J* = 20.7 Hz, 1F), –159.36 (td, *J* = 20.7 Hz, *J* = 10.3 Hz, 1F, *meta*-F), –160.01 (m, 2F), –160.18 (td, *J* = 24.2 Hz, *J* = 6.9 Hz, 1F, *meta*-F), –160.44 (td, *J* = 20.7 Hz, J = 6.9 Hz, 1F, *meta*-F), –160.70 (td, *J* = 24.2 Hz, *J* = 10.3 Hz, 1F), –161.93 (td, *J* = 24.2 Hz, J = 6.9 Hz, 1F, *meta*-F), –162.34 (t, *J* = 20.7 Hz, 1F, *meta*-F), –163.16 (t, *J* = 24.2 Hz, 1F, *meta*-F), and –163.61 (t, *J* = 20.7 Hz, 1F) ppm; ^{31}P NMR (242.95 MHz, $CDCl_3$, 25 °C): δ = –2.68 (s) ppm. UV/vis: $\lambda_{max}(CH_2Cl_2)$/nm 326 (ε/dm^3 mol^{-1} cm^{-1} 49000), 393 (56000), 480 (16000), 560 (sh, 8800), and 780 (3300) nm. HRMS (ESI-TOF, positive) calcd. for $C_{55}H_9F_{24}N_5PO$ $[M+H]^+$ 1242.0156; found 1242.0142.

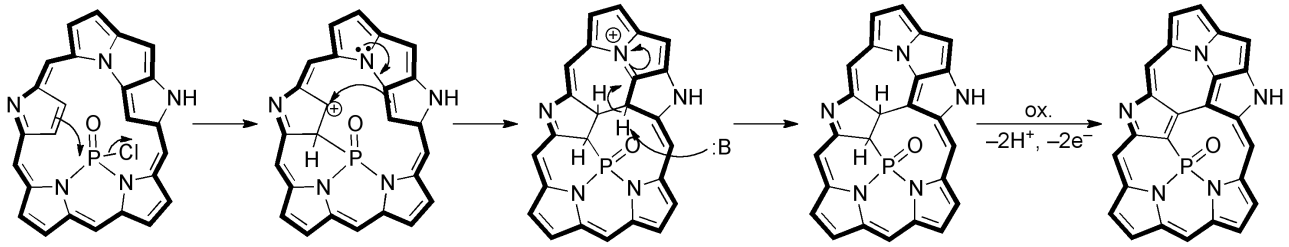

Scheme S1. The plausible mechanism of *β*-*β* bond formation.

3. High-Resolution ESI-MS

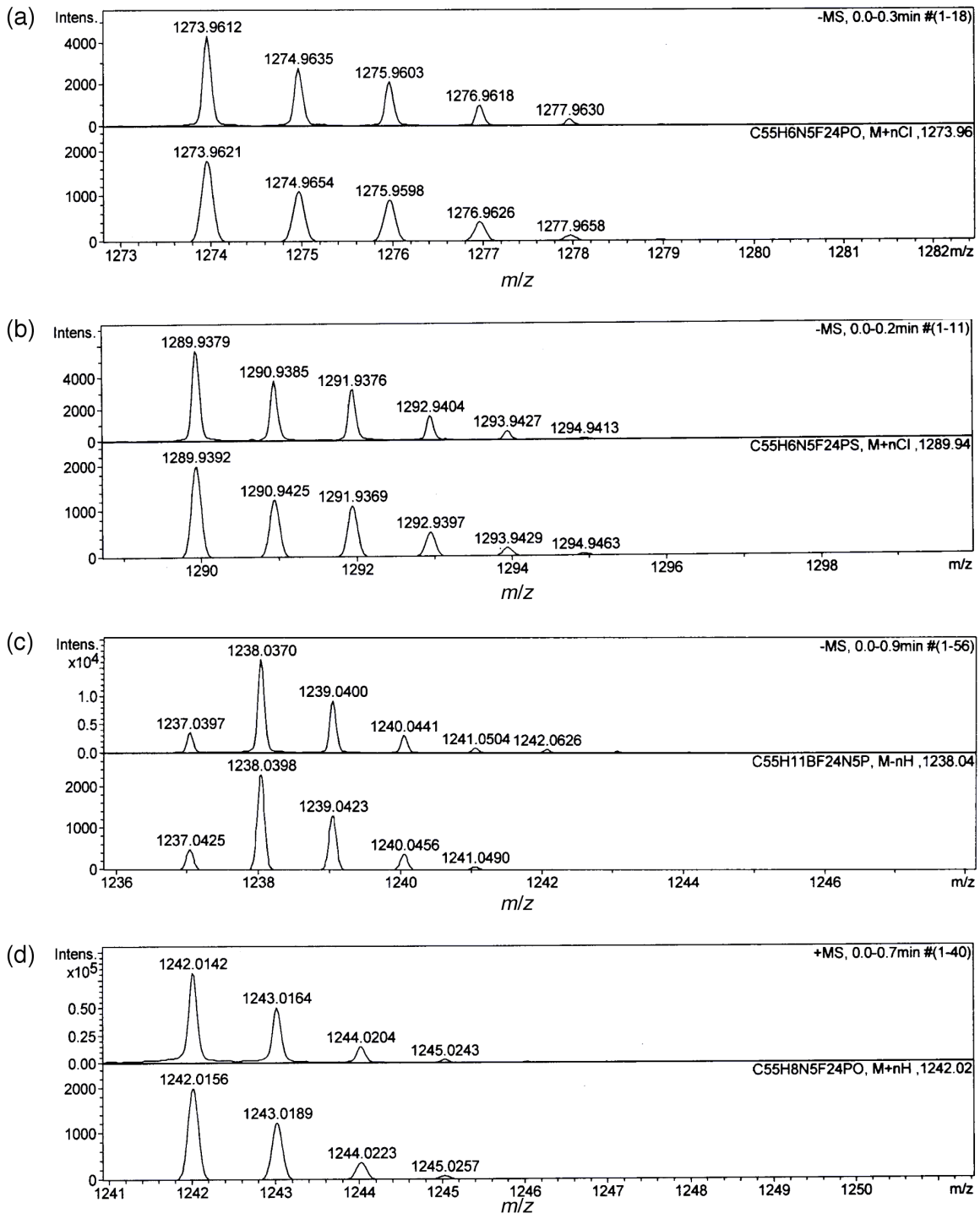

Figure S1. Observed (top) and simulated (bottom) high-resolution ESI-MS of (a) **2**, (b) **3**, (c) **4**, and (d) **5**.

4. UV/Vis Absorption Spectra

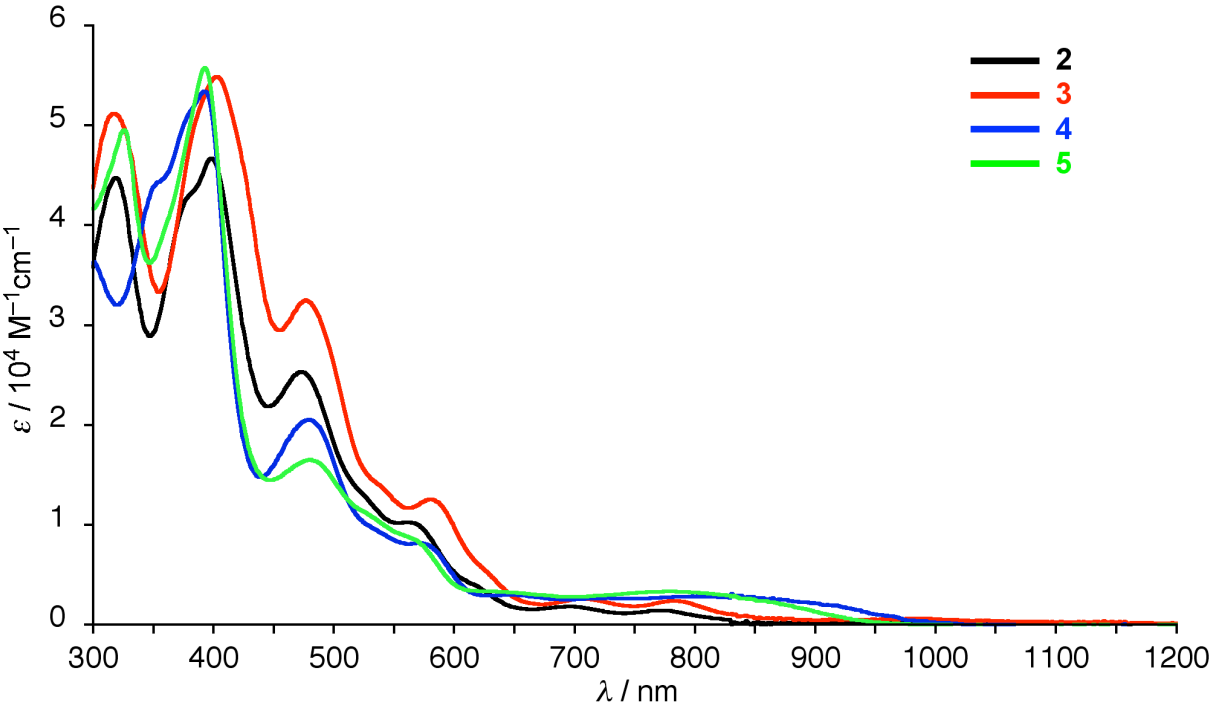

Figure S2. UV / Vis absorption spectra of **2** (black), **3** (red), **4** (blue) and **5** (green) in CH_2Cl_2.

5. NMR Spectra

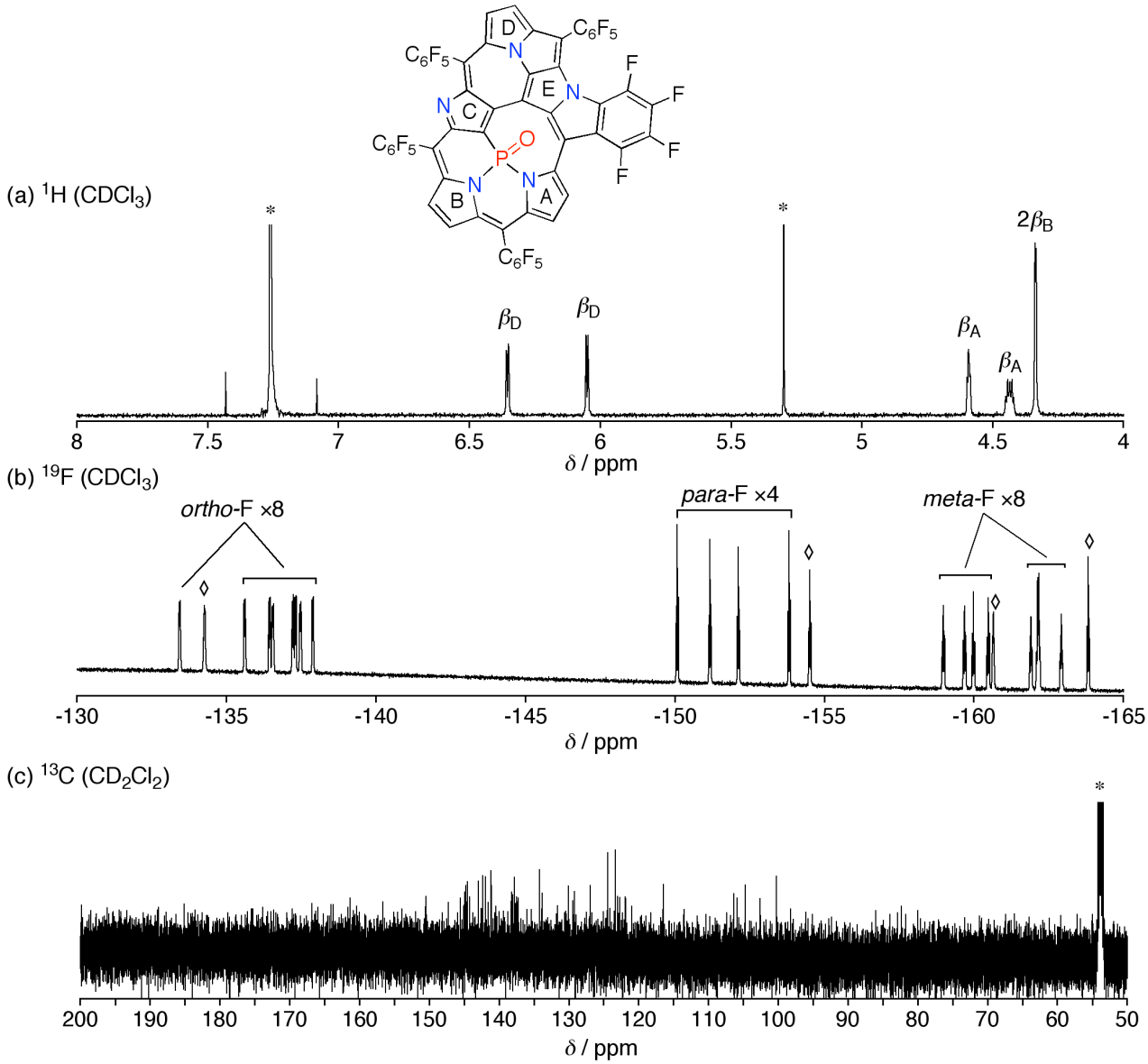

Figure S3. (a) ^{1}H, (b) ^{19}F and (c) ^{13}C NMR spectra of **2** at 25 °C. Peaks marked with ∗ are due to residual solvents and impurities. Peaks marked with ◊ are signals of fluorine atoms at the *N*-fused aryl substituent.

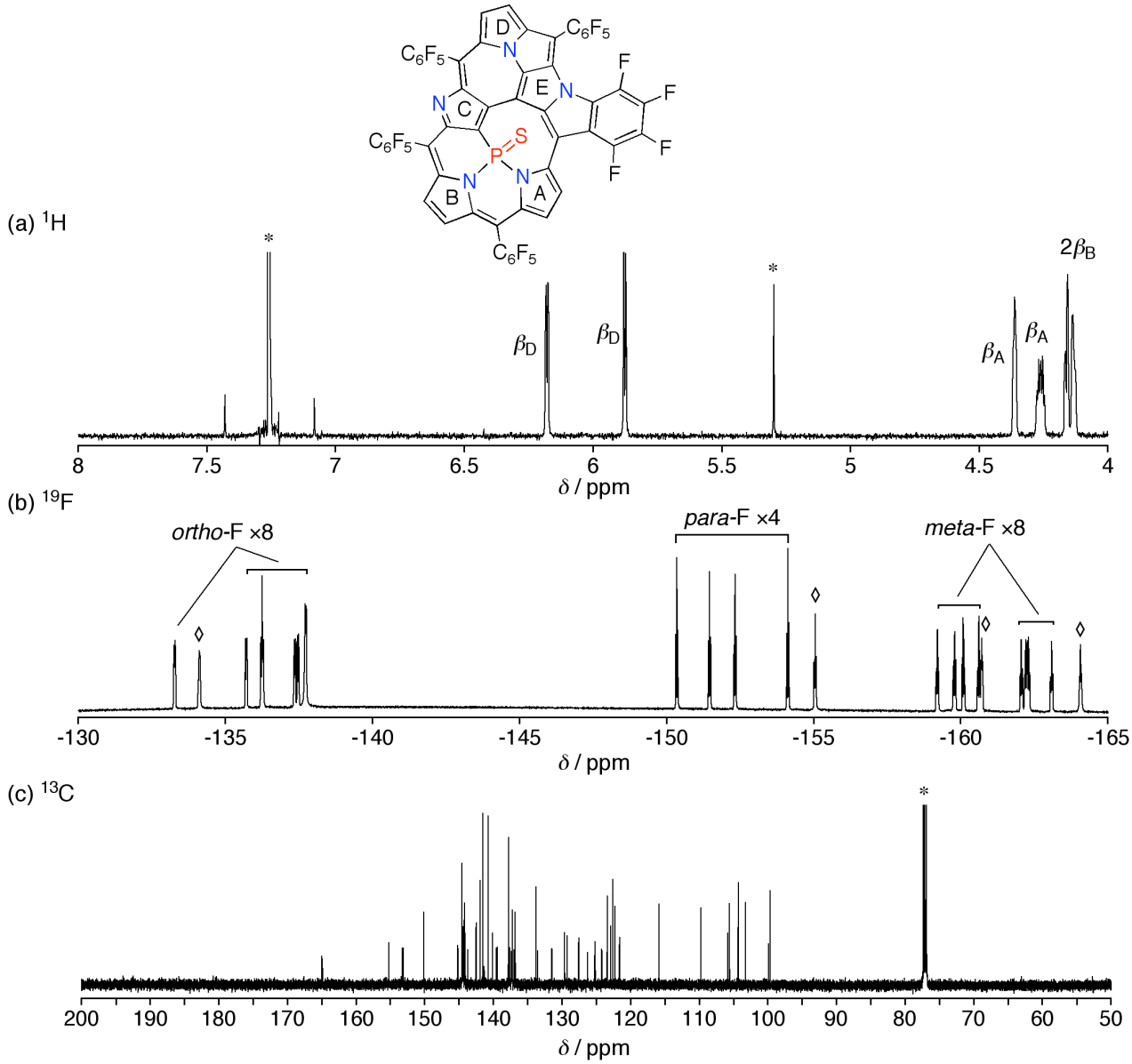

Figure S4. (a) ^{1}H, (b) ^{19}F and (c) ^{13}C NMR spectra of **3** in $CDCl_3$ at 25 °C. Peaks marked with ∗ are due to residual solvents and impurities. Peaks marked with ◊ are signals of fluorine atoms at the *N*-fused aryl substituent.

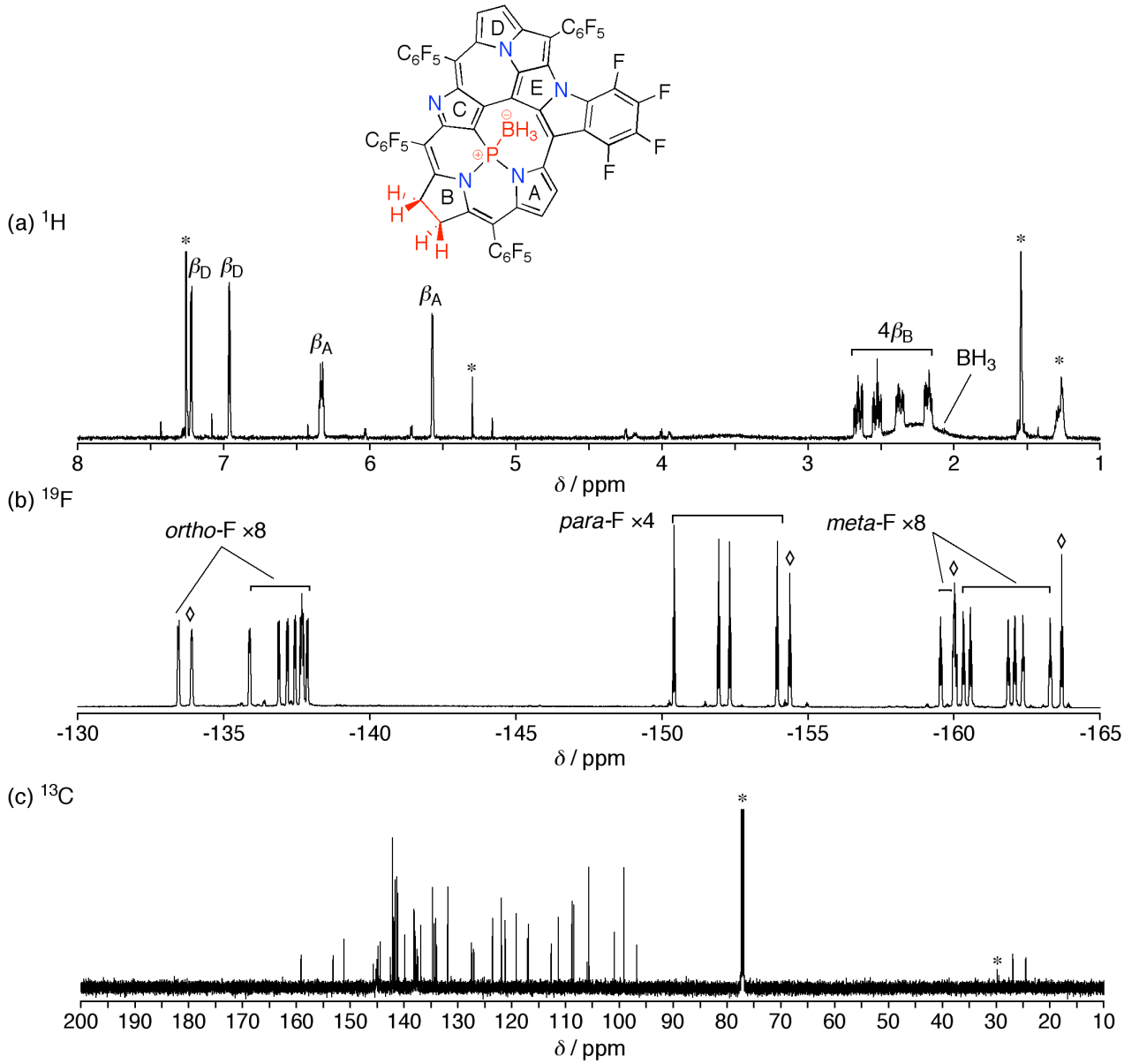

Figure S5. (a) ^{1}H, (b) ^{19}F and (c) ^{13}C NMR spectra of **4** in $CDCl_3$ at 25 °C. Peaks marked with ∗ are due to residual solvents and impurities. Peaks marked with ◊ are signals of fluorine atoms at the *N*-fused aryl substituent.

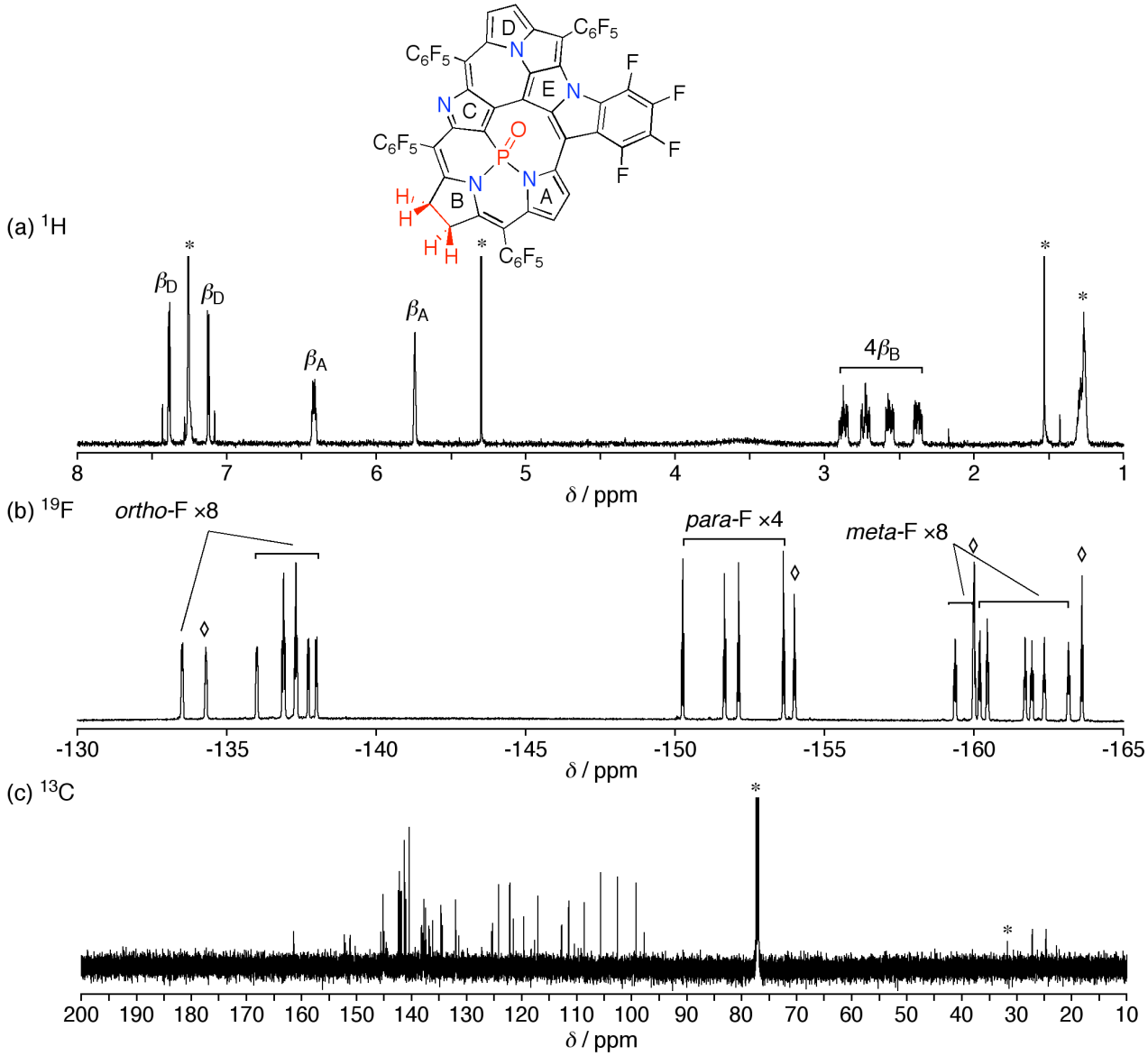

Figure S6. (a) ^{1}H, (b) ^{19}F and (c) ^{13}C NMR spectra of **5** in $CDCl_3$ at 25 °C. Peaks marked with ∗ are due to residual solvents and impurities. Peaks marked with ◊ are signals of fluorine atoms at the *N*-fused aryl substituent.

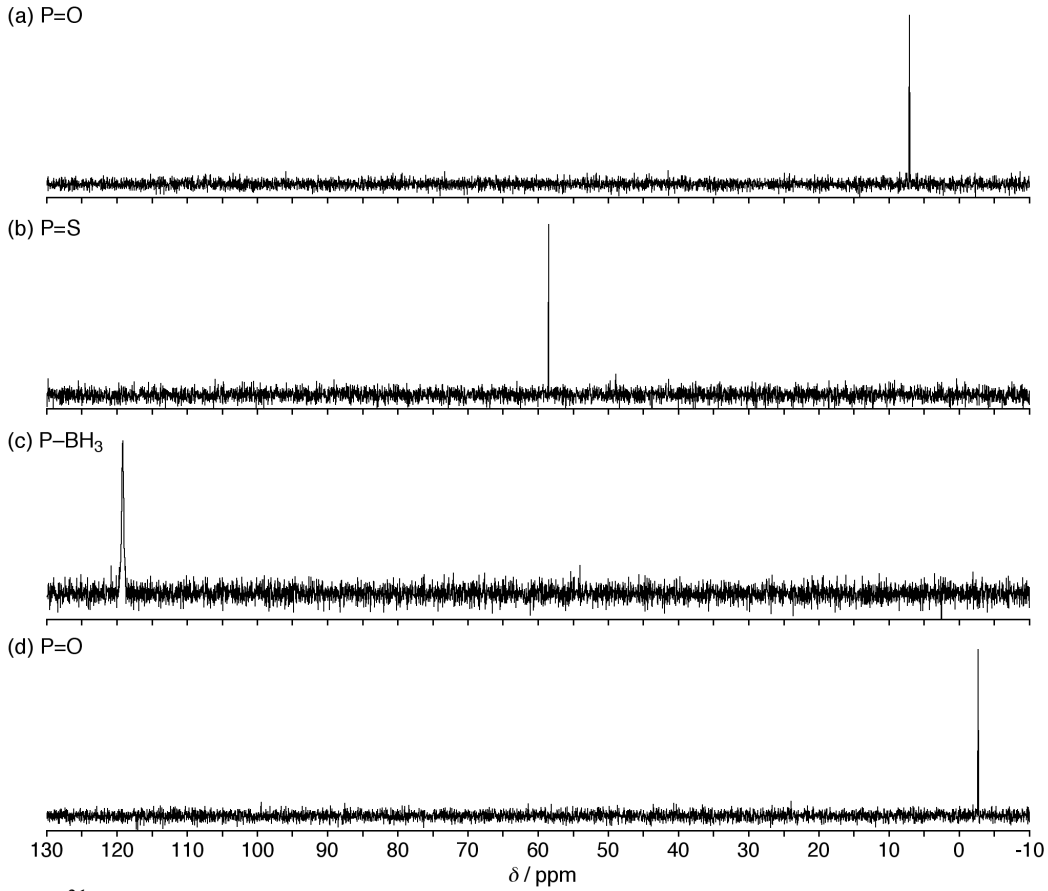

Figure S7. ^{31}P NMR spectra of (a) **2**, (b) **3**, (c) **4**, and (d) **5** in $CDCl_3$ at 25 °C.

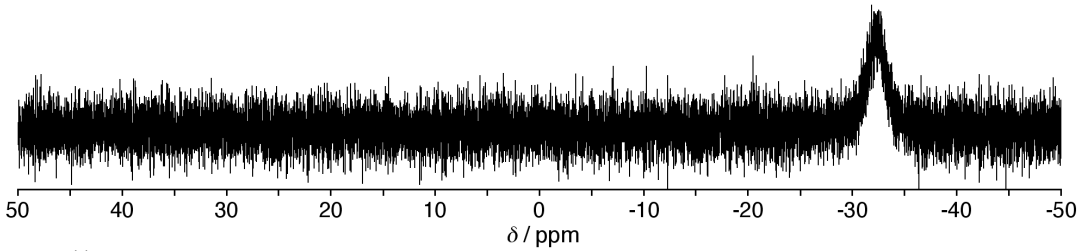

Figure S8. ^{11}B NMR spectrum of **4** in $CDCl_3$ at 25 °C.

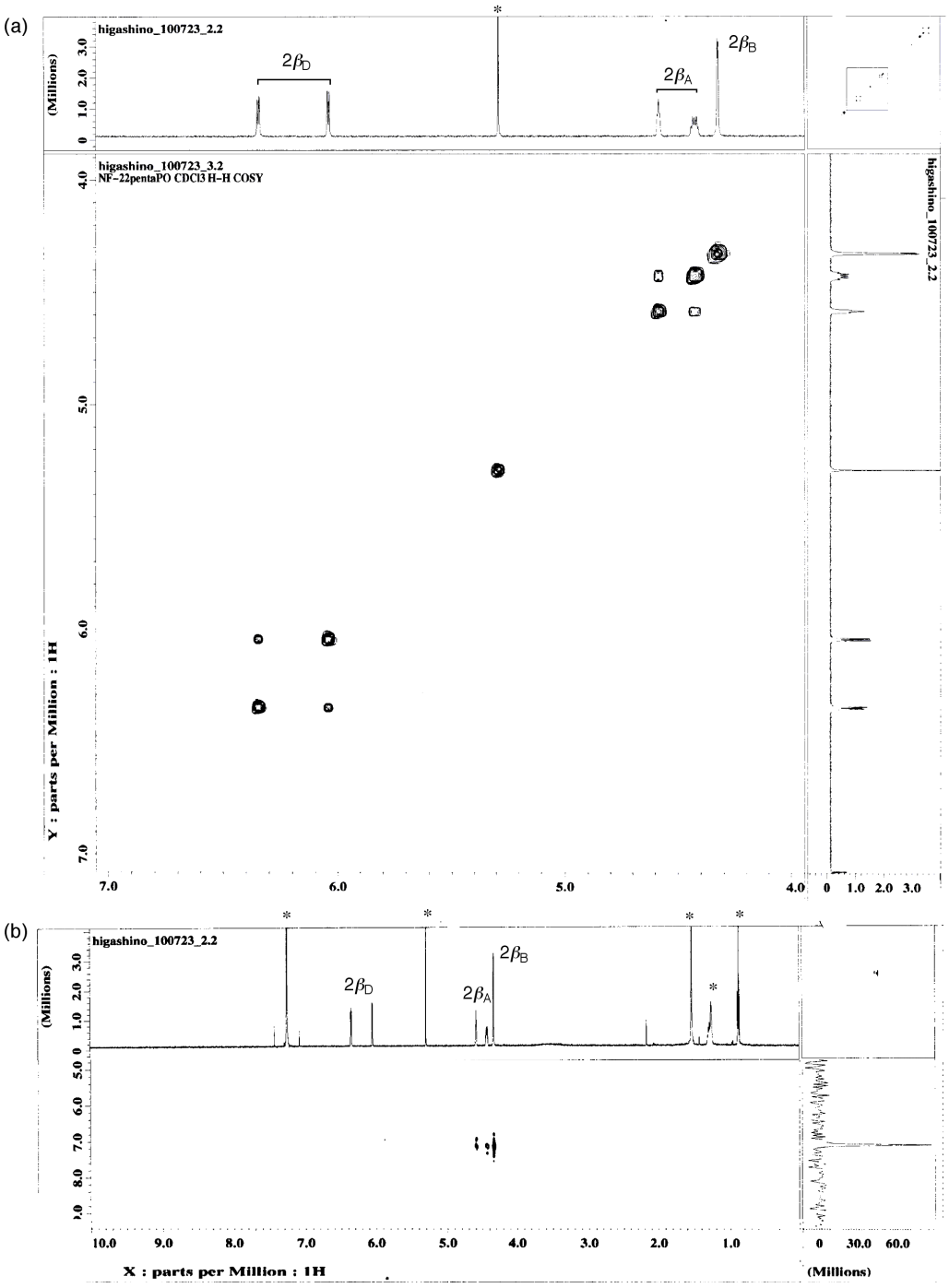

Figure S9. (a) ^{1}H–^{1}H COSY and (b) ^{1}H–^{31}P HMBC NMR spectra of **2** in $CDCl_3$ at 25 °C. Peaks marked with ∗ are due to residual solvents and impurities.

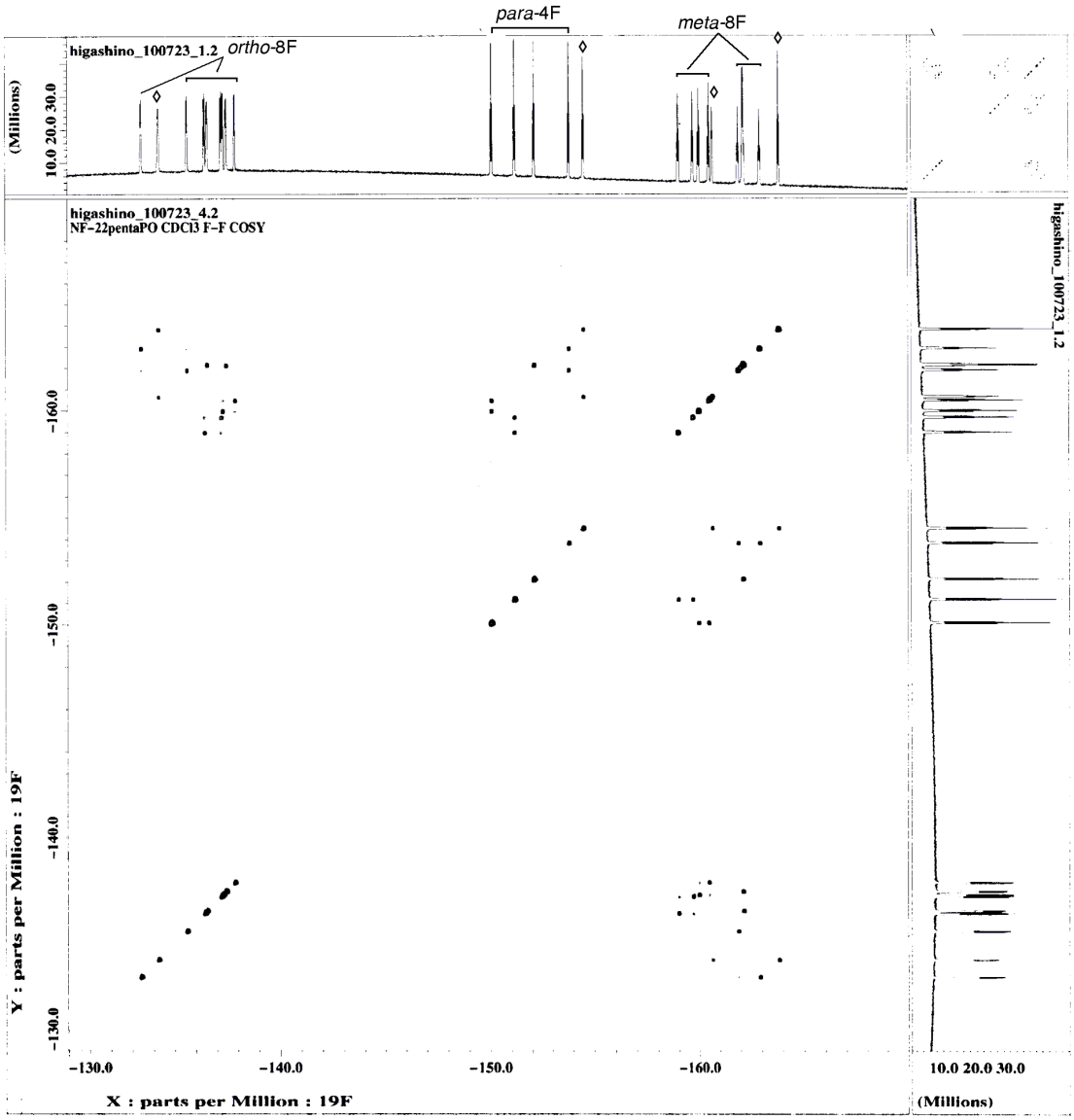

Figure S10. ^{19}F–^{19}F COSY NMR spectrum of **2** in $CDCl_3$ at 25 °C. Peaks marked with ◊ are signals of fluorine atoms at the *N*-fused aryl substituent.

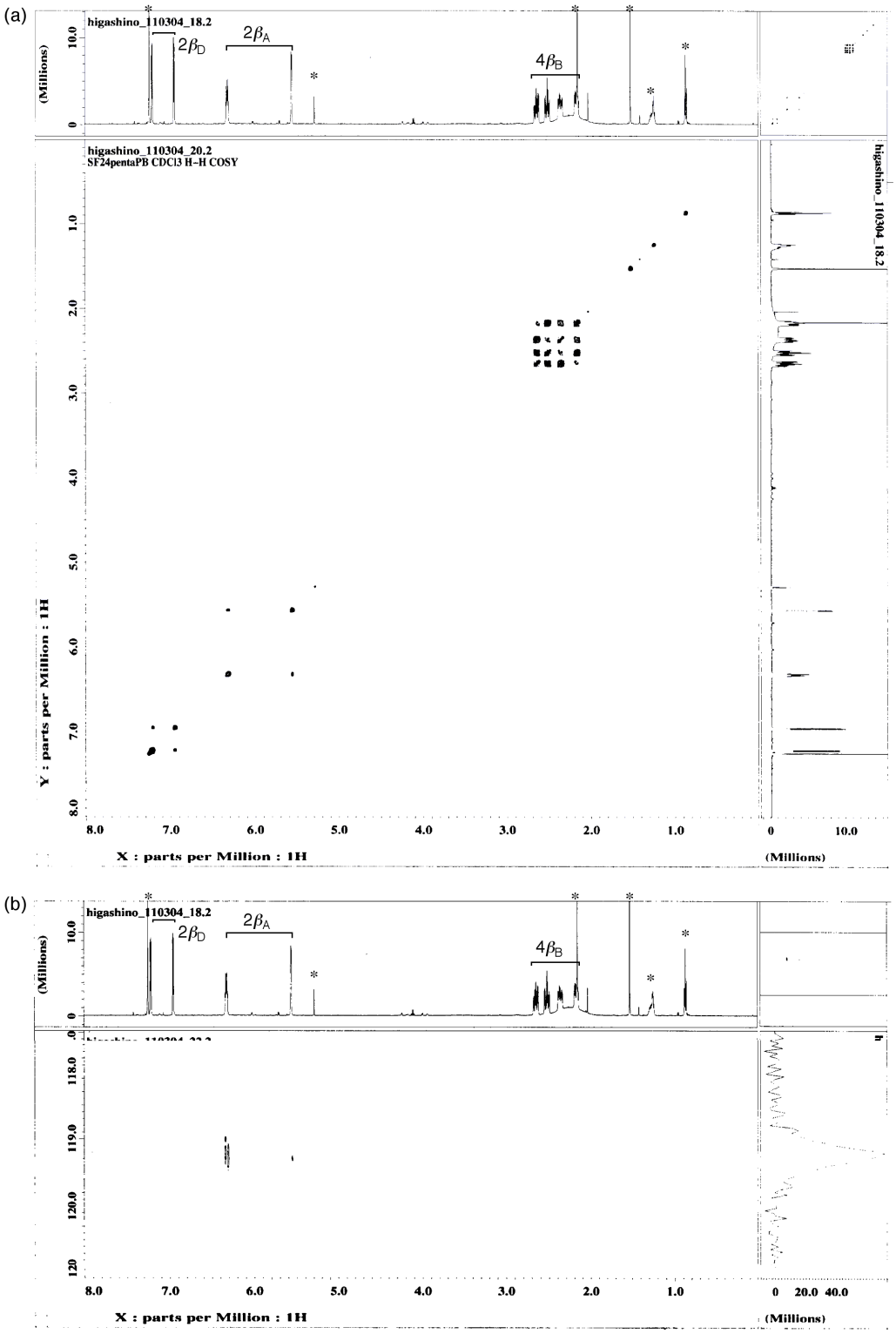

Figure S11. (a) ^{1}H–^{1}H COSY and (b) ^{1}H–^{31}P HMBC NMR spectra of **4** in $CDCl_3$ at 25 °C. Peaks marked with ∗ are due to residual solvents and impurities.

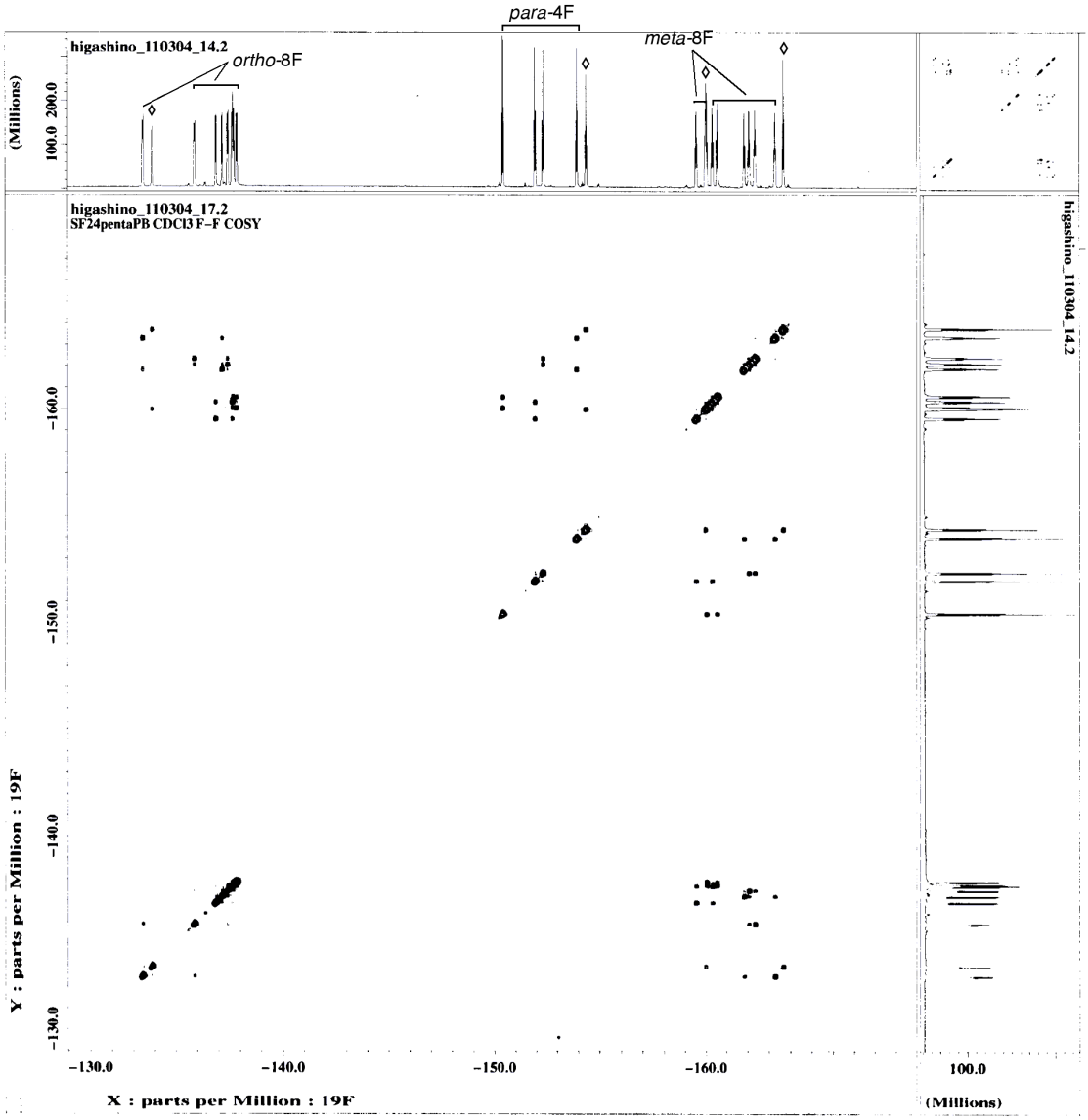

Figure S12. ^{19}F–^{19}F COSY NMR spectrum of **4** in $CDCl_3$ at 25 °C. Peaks marked with ◊ are signals of fluorine atoms at the *N*-fused aryl substituent.

6. Cyclic Voltammograms

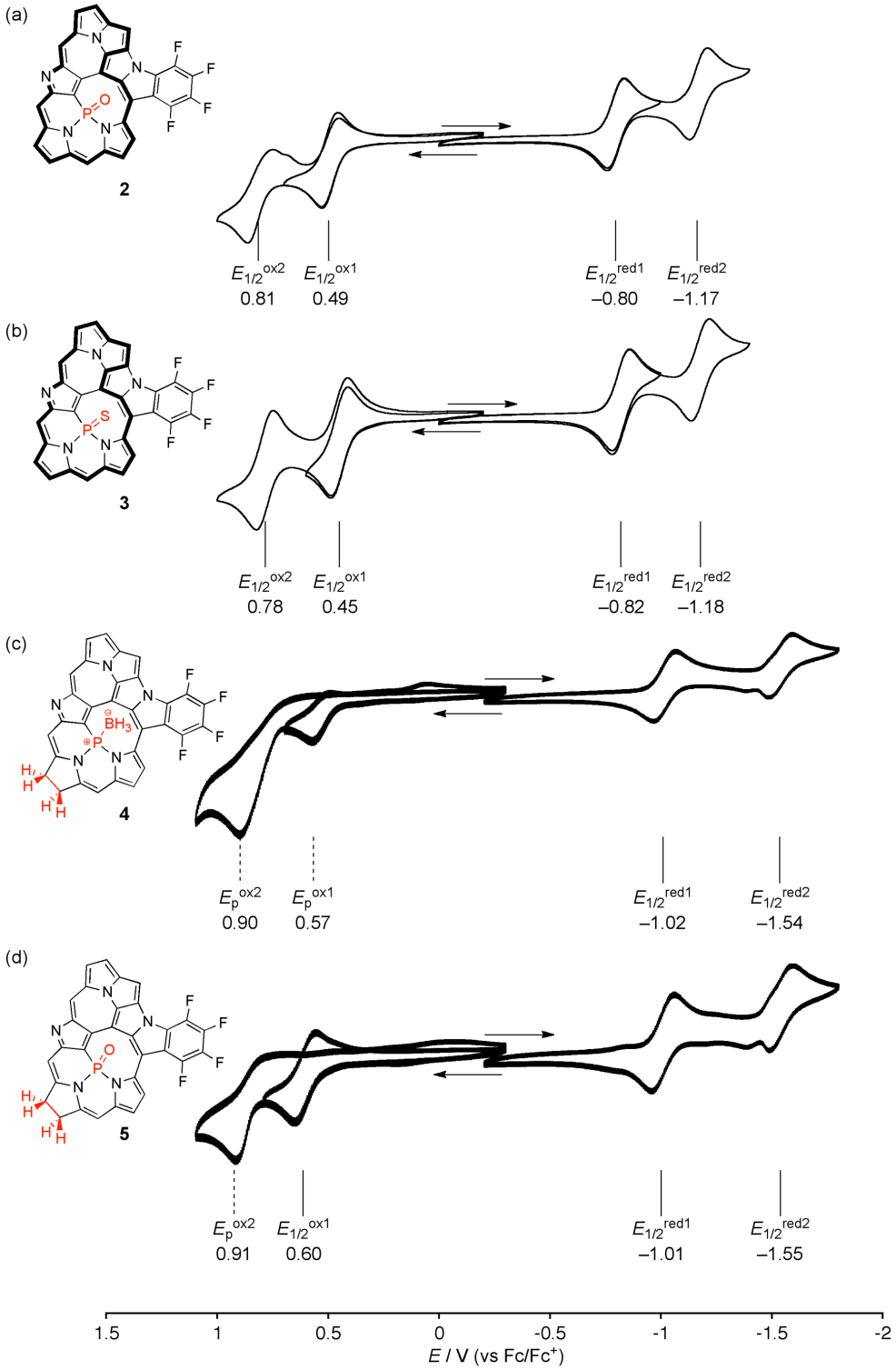

Figure S13. Cyclic voltammograms of (a) **2**, (b) **3**, (c) **4**, and (d) **5**. Cyclic voltammograms are measured in the following conditions; solvent: CH_2Cl_2; scan rate: (a, b) 0.05 Vs^{-1}, (c, d) 0.1 Vs^{-1}; working electrode: glassy carbon; reference electrode: $Ag/AgClO_4$; electrolyte: Bu_4NPF_6.

7. X-Ray Crystallographic Details

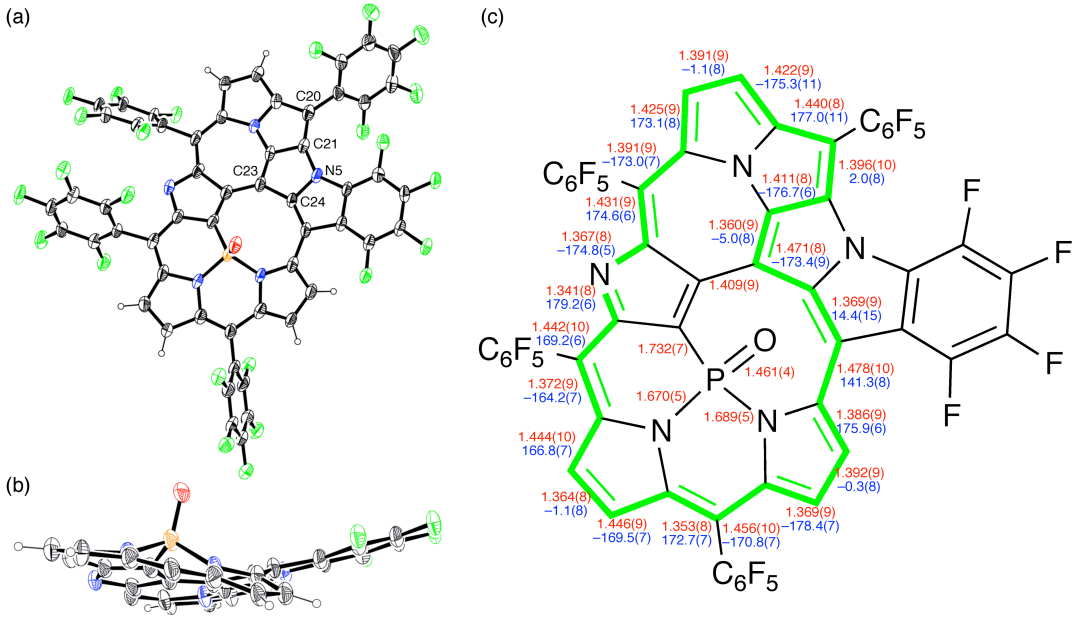

Figure S14. X-Ray crystal structure of **2**: (a) top view and (b) side view. Thermal ellipsoids represents 30% probability and solvent molecules are omitted for clarity. In the side view, *meso*-pentafluorophenyl substituents are omitted for clarity. (c) Detailed structural data of **2**. The conjugated 24π-electron circuit (green), along which bond lengths in Å (numbers in red), and dihedral angles in deg (numbers in blue) are indicated. (These values are one of the two molecules in the unit cell.)

PLAT723_Alert_1_A of **2:** The bond length of C(20)–C(21), C(21)–N(5), N(5)–C(24), C(74)–C(75), C(75)–C(76), and C(76)–N(10) are 1.396(10), 1.412(8), 1.414(8), 1.443(9), 1.407(11), and 1.420(9) Å, respectively. In addition, C(23)–C(24) and C(78)–C(79) distances are 1.471(8) and 1.452(9) Å, which are likely C–C single bond. Probably, the CIF check program regarded the C(20)–C(21)–N(5)–C(24) and C(74)–C(75)–C(76)–N(10) as the sp^3-hybridized moiety, so that the Alert A may be reported.

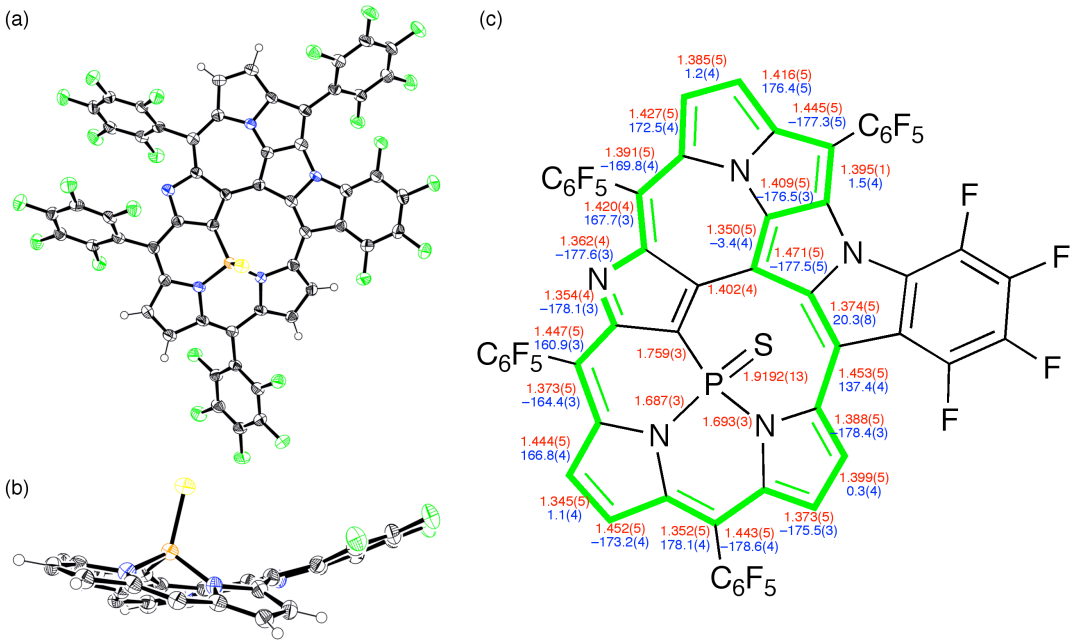

Figure S15. X-Ray crystal structure of **3**: (a) top view and (b) side view. Thermal ellipsoids represents 50% probability and solvent molecules are omitted for clarity. In the side view, *meso*-pentafluorophenyl substituents are omitted for clarity. (c) Detailed structural data of **3**. The conjugated 24π-electron circuit (green), along which bond lengths in Å (numbers in red), and dihedral angles in deg (numbers in blue) are indicated.

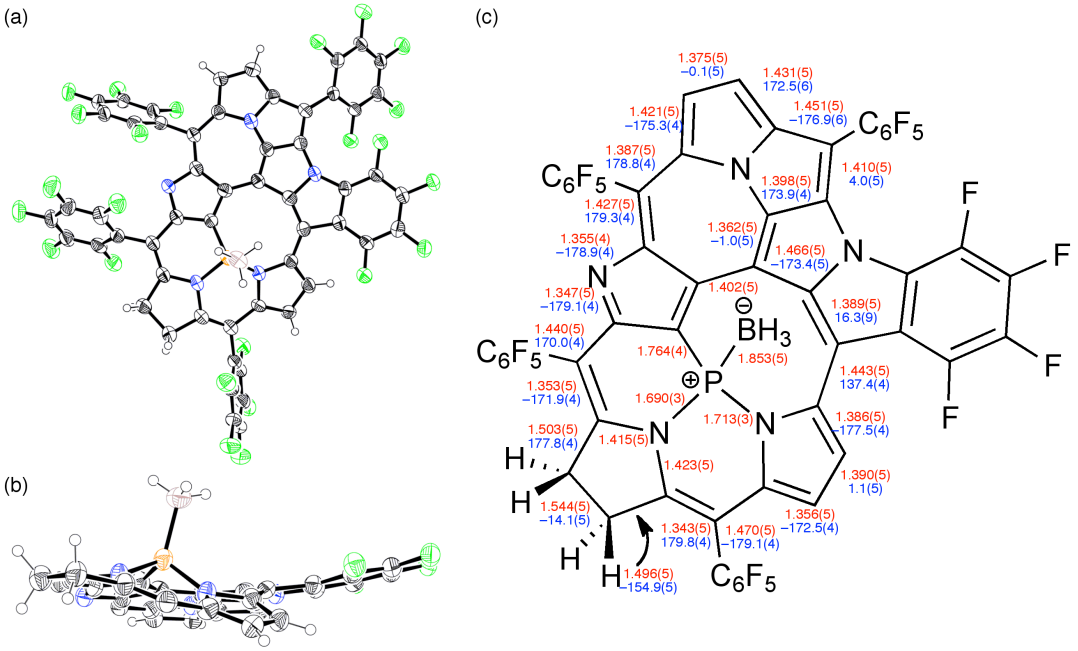

Figure S16. X-Ray crystal structure of **4**: (a) top view and (b) side view. Thermal ellipsoids represents 50% probability and solvent molecules are omitted for clarity. In the side view, *meso*-pentafluorophenyl substituents are omitted for clarity. (c) Detailed structural data of **4**. The bond lengths in Å (numbers in red), and dihedral angles in deg (numbers in blue) are indicated.

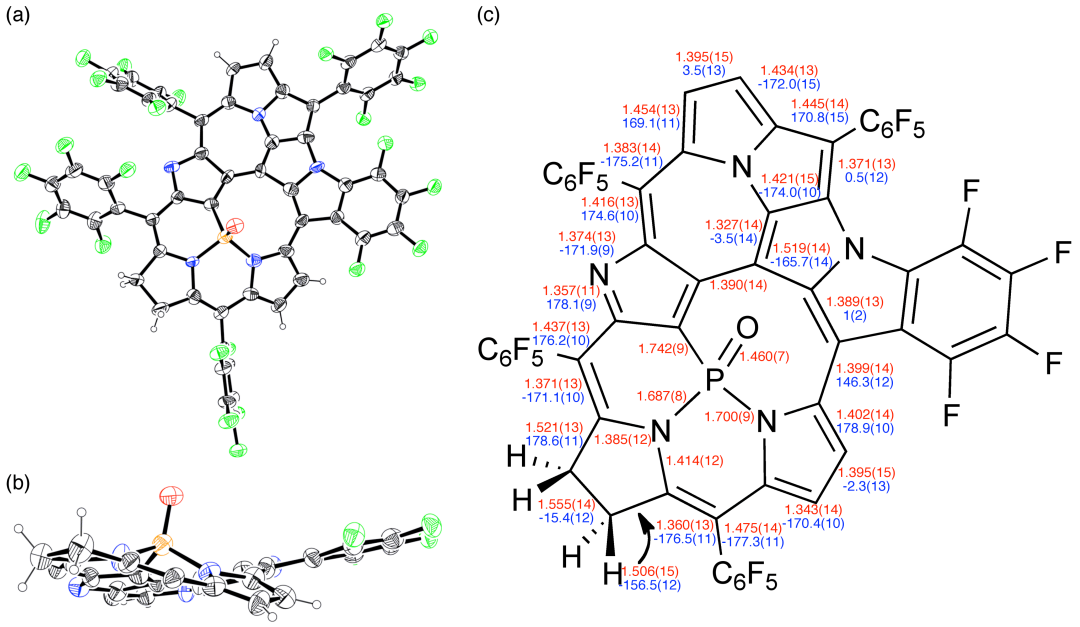

Figure S17. X-Ray crystal structure of **5**: (a) top view and (b) side view. Thermal ellipsoids represents 30% probability and solvent molecules are omitted for clarity. In the side view, *meso*-pentafluorophenyl substituents are omitted for clarity. (c) Detailed structural data of **5**. The bond lengths in Å (numbers in red), and dihedral angles in deg (numbers in blue) are indicated.

Table S1. Crystal data of **2**, **3**, **4** and **5**.

	2	**3**	**4**	**5**
formula	$4(C_{55}H_6F_{24}N_5OP)\cdot 13(C_6H_5Cl)$	$C_{55}H_6F_{24}N_5PS\cdot 3(C_7H_8)$	$2(C_{55}H_{11}BF_{24}N_5P)\cdot 3(C_6H_{14})\cdot C_7H_8$	$C_{55}H_8F_{24}N_5OP\cdot C_2H_3N\cdot 0.75(CCl_4)\cdot 0.5$(water)
M_r	6421.63	1532.09	2829.59	1405.92
T [K]	93(2)	93(2)	93(2)	93(2)
crystal system	monoclinic	monoclinic	monoclinic	triclinic
space group	$P2_1/a$ (No.14)	$P2_1/c$ (No.14)	$C2/c$ (No.15)	P-1 (No.2)
a [Å]	29.5322(5)	19.4591(5)	30.1073(6)	10.1849(5)
b [Å]	10.3705(2)	8.6913(2)	18.0820(3)	14.9773(8)
c [Å]	41.5808(8)	37.1609(11)	22.4608(4)	17.6759(10)
α [°]	90	90	90	85.568(3)
β [°]	99.1602(8)	94.5998(18)	106.2569(10)	88.271(3)
γ [°]	90	90	90	76.766(3)
V [Å^3]	12572.3(4)	6264.6(3)	11738.8(4)	2616.7(2)
Z	2	4	4	2
ρ_{calcd} [g cm^{-3}]	1.696	1.624	1.601	1.784
R_1 [$I > 2\sigma(I)$]	0.0993	0.0675	0.0759	0.1190
wR_2 [all data]	0.2961	0.1500	0.1619	0.3747
GOF	0.988	1.057	1.001	1.076
CCDC number	827555	827556	827554	842955

8. DFT Calculations

All calculations were carried out using the *Gaussian 09* program.[S1] Initial geometries were obtained from X-ray structures. All structures were fully optimized without any symmetry restriction. The calculations were performed by the density functional theory (DFT) method with restricted B3LYP (Becke's three-parameter hybrid exchange functionals and the Lee-Yang-Parr correlation functional) level,[S2,S3] employing a basis set 6-31G(d) for C, H, N, F, P, O, S and B. The NICS values and absolute ^{1}H shielding values were obtained with the GIAO method at the B3LYP/6-31G(d) level. The ^{1}H chemical shift values were calculated relative to $CHCl_3$ (δ = 7.26 ppm, absolute shielding: 24.94 ppm). The global ring centers for the NICS values were designated at the nonweighted means of the carbon and nitrogen coordinates on the peripheral positions of macrocycles. In addition, NICS values were also calculated on centres of other local cyclic structures as depicted in the following figures. Excitation energies and oscillator strengths for the crystal and optimized structures were calculated with the TD-SCF method at the B3LYP/6-31G(d) level.

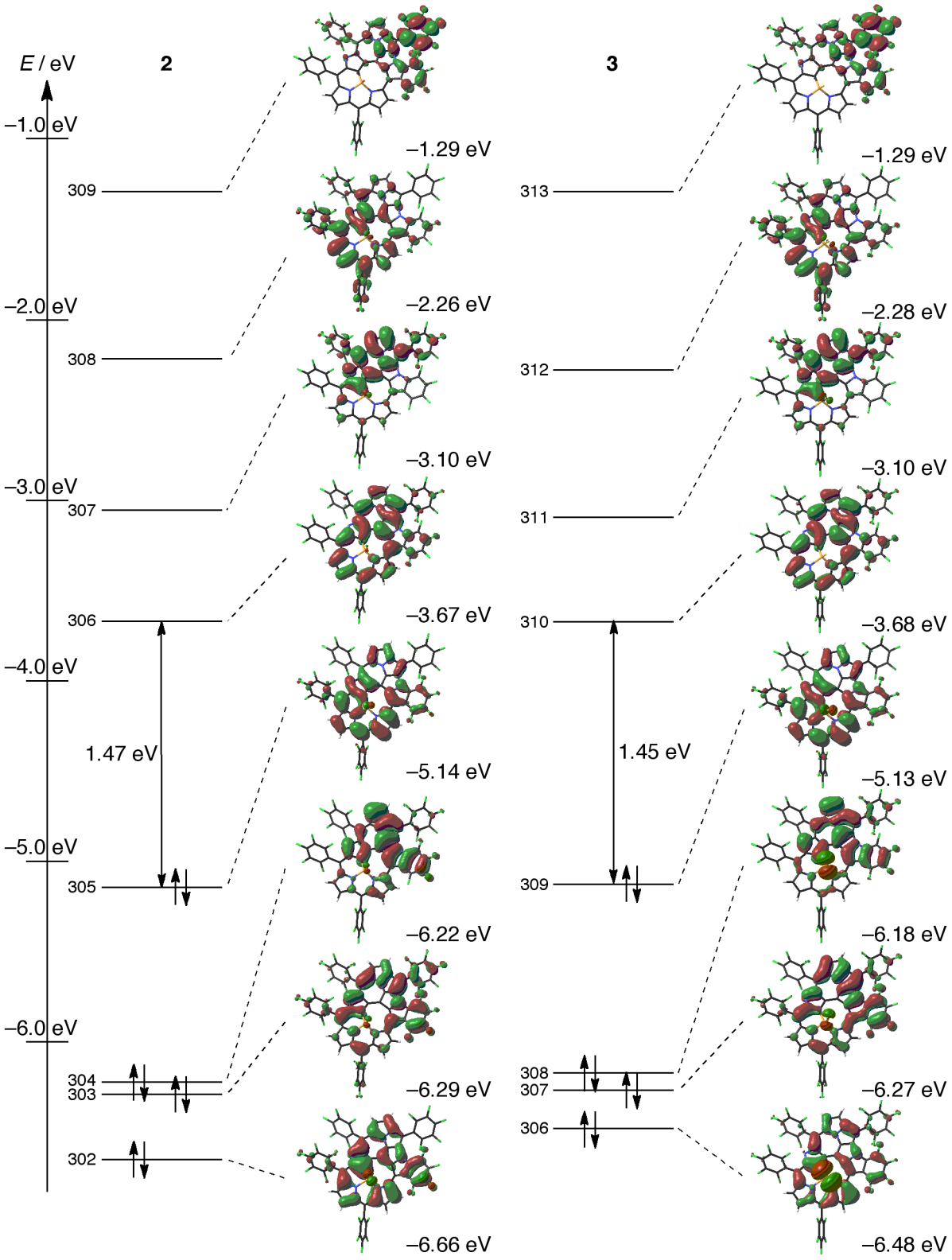

Figure S18. Selected molecular orbitals of **2** and **3** on the optimized structures.

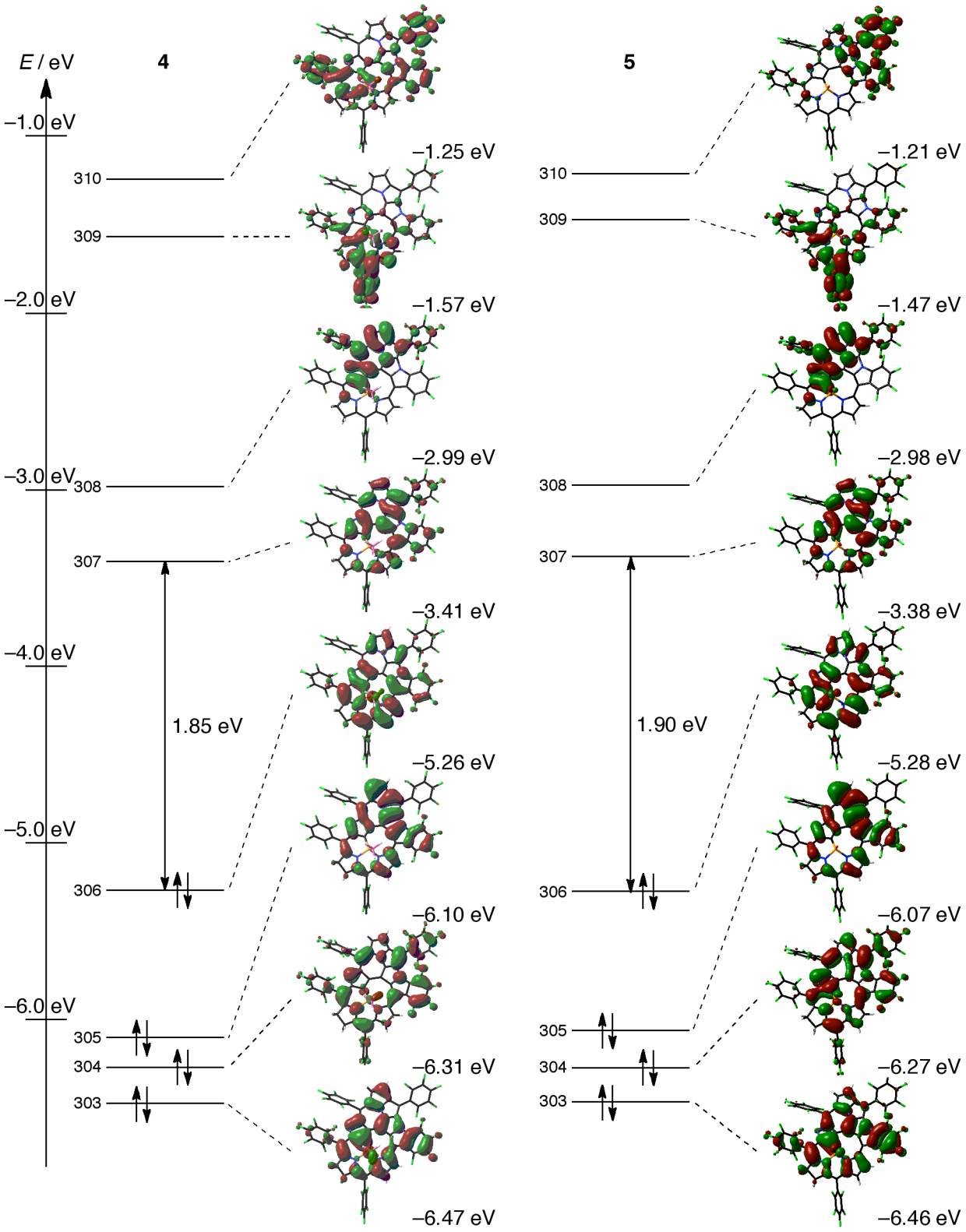

Figure S19. Selected molecular orbitals of **4** and **5** on the optimized structures.

(a)

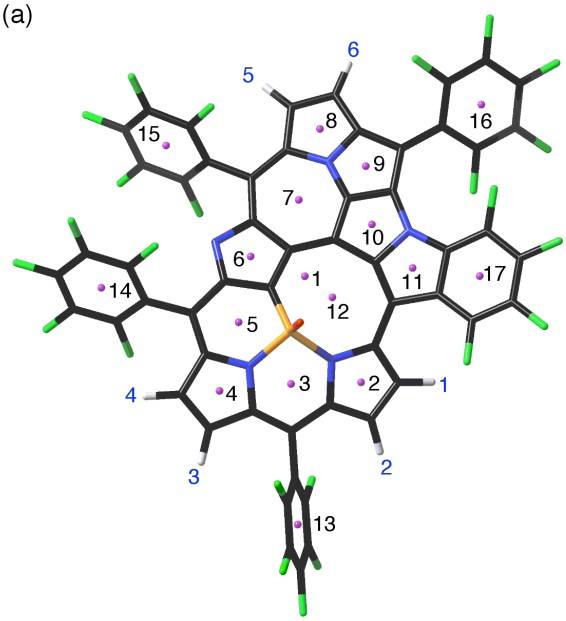

position	NICS (ppm)	^{1}H	δ (ppm)
1	23.09	1	2.42
2	2.61	2	3.08
3	24.43	3	2.25
4	12.26	4	2.30
5	25.43	5	4.68
6	–5.25	6	5.05
7	0.68		
8	–3.49		
9	5.01		
10	11.38		
11	–4.14		
12	30.96		
13	–17.00		
14	–17.14		
15	–16.44		
16	–16.12		
17	–12.34		

(b)

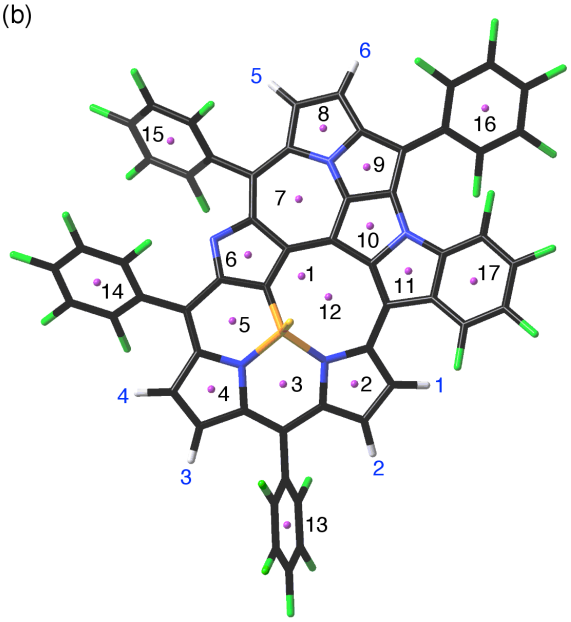

position	NICS (ppm)	^{1}H	δ (ppm)
1	22.80	1	2.35
2	3.26	2	2.94
3	25.29	3	2.11
4	12.24	4	2.14
5	26.51	5	4.55
6	–5.12	6	4.93
7	1.57		
8	–2.83		
9	5.66		
10	11.04		
11	–4.30		
12	29.86		
13	–17.10		
14	–17.20		
15	–16.50		
16	–16.15		
17	–12.40		

Figure S20. NICS values at various positions and simulated chemical shifts of (a) **2** and (b) **3** based on the optimized structures.

(a)

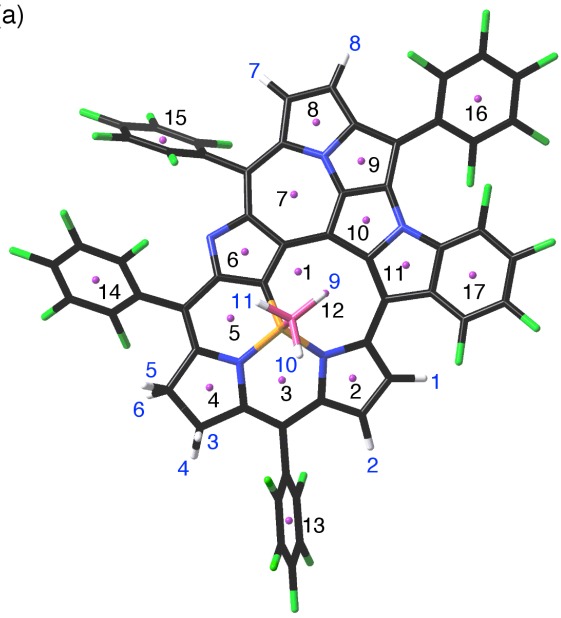

position	NICS (ppm)	^{1}H	δ (ppm)
1	0.17	1	5.90
2	–6.85	2	5.33
3	7.80	3	2.20
4	–6.67	4	1.41
5	9.32	5	2.00
6	–9.88	6	2.24
7	–4.95	7	6.44
8	–8.96	8	4.78
9	–4.55	9	3.64
10	5.64	10	3.45
11	–4.07	11	3.22
12	9.67		
13	–15.87		
14	–15.89		
15	–15.44		
16	–15.21		
17	–12.98		

(b)

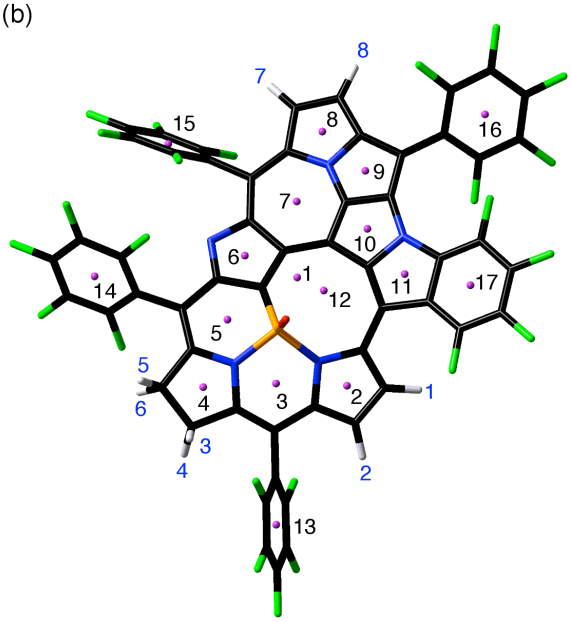

position	NICS (ppm)	^{1}H	δ (ppm)
1	0.98	1	5.81
2	–6.74	2	5.29
3	5.54	3	2.36
4	–6.32	4	1.63
5	6.62	5	2.16
6	–10.59	6	2.34
7	–6.12	7	6.56
8	–9.68	8	6.88
9	–5.52		
10	6.08		
11	–3.80		
12	10.05		
13	–15.79		
14	–15.85		
15	–15.36		
16	–15.16		
17	–12.89		

Figure S21. NICS values at various positions and simulated chemical shifts of (a) **4** and (b) **5** based on the optimized structures.

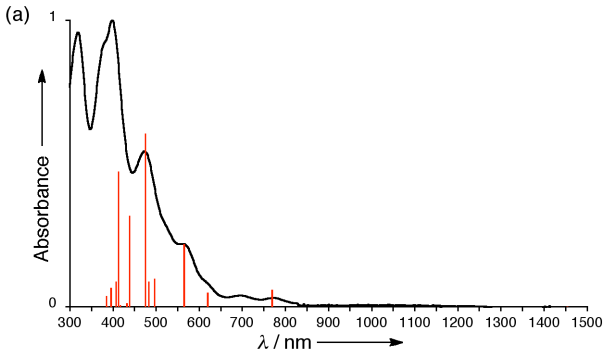

λ [nm]	*f*
1457	0.0004
770	0.0355
620	0.0296
565	0.1315
496	0.0586
484	0.0525
475	0.3624
438	0.1906
433	0.0075
417	0.0034
412	0.2831
407	0.0522
396	0.0397
388	0.0005
384	0.0228

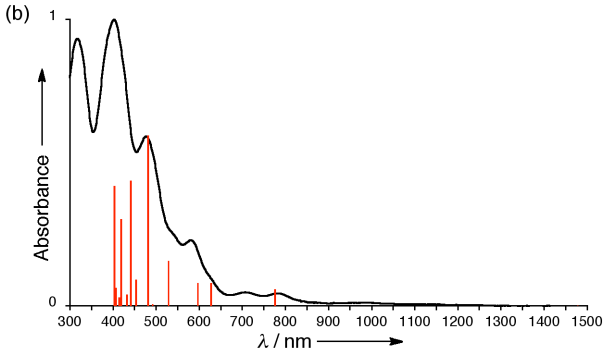

λ [nm]	*f*
1482	0.0004
777	0.0342
628	0.0470
597	0.0473
529	0.0937
492	0.0029
482	0.3567
476	0.0349
453	0.0543
441	0.2618
432	0.0235
419	0.1812
414	0.0172
408	0.0371
403	0.2507

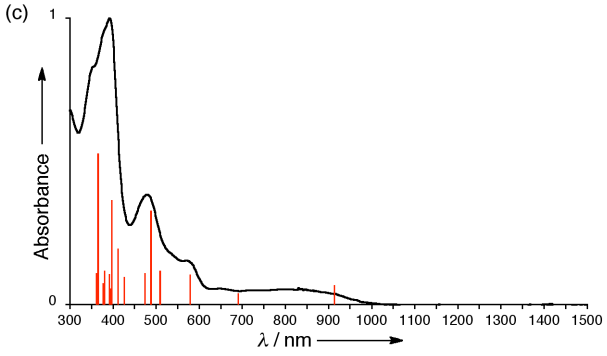

λ [nm]	*f*
915	0.0399
691	0.0232
579	0.0631
509	0.0712
488	0.1962
473	0.0662
426	0.0581
411	0.1173
397	0.2187
393	0.0337
392	0.0638
380	0.0708
377	0.0443
365	0.3168
361	0.0656

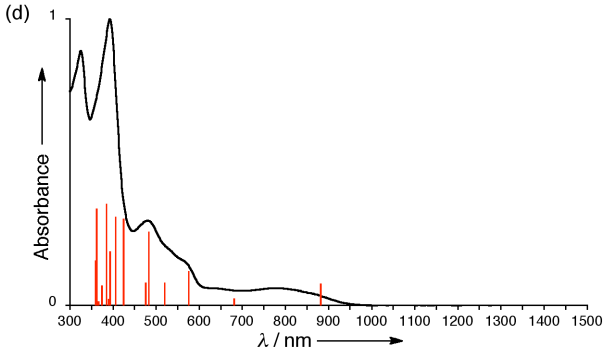

λ [nm]	*f*
883	0.0456
682	0.0144
576	0.0714
520	0.0475
483	0.1540
476	0.0480
424	0.1817
406	0.1856
393	0.1134
389	0.0131
384	0.2126
374	0.0412
366	0.0083
361	0.2024
360	0.0938

Figure S22. Calculated absorption spectra on the basis of optimized structures (bar) and observed absorption spectra (line) of (a) **2**, (b) **3**, (c) **4**, and (d) **5**.

9. References

[S1] S. Mori, J.-Y. Shin, S. Shimizu, F. Ishikawa, H. Furuta, A. Osuka, *Chem. Eur. J.*, 2005, **11**, 2417–2425.

[S2] Gaussian 09, Revision A.02, M. J. Frisch, G. W. Trucks, H. B. Schlegel, G. E. Scuseria, M. A. Robb, J. R. Cheeseman, G. Scalmani, V. Barone, B. Mennucci, G. A. Petersson, H. Nakatsuji, M. Caricato, X. Li, H. P. Hratchian, A. F. Izmaylov, J. Bloino, G. Zheng, J. L. Sonnenberg, M. Hada, M. Ehara, K. Toyota, R. Fukuda, J. Hasegawa, M. Ishida, T. Nakajima, Y. Honda, O. Kitao, H. Nakai, T. Vreven, J. A. Montgomery, Jr., J. E. Peralta, F. Ogliaro, M. Bearpark, J. J. Heyd, E. Brothers, K. N. Kudin, V. N. Staroverov, R. Kobayashi, J. Normand, K. Raghavachari, A. Rendell, J. C. Burant, S. S. Iyengar, J. Tomasi, M. Cossi, N. Rega, J. M. Millam, M. Klene, J. E. Knox, J. B. Cross, V. Bakken, C. Adamo, J. Jaramillo, R. Gomperts, R. E. Stratmann, O. Yazyev, A. J. Austin, R. Cammi, C. Pomelli, J. W. Ochterski, R. L. Martin, K. Morokuma, V. G. Zakrzewski, G. A. Voth, P. Salvador, J. J. Dannenberg, S. Dapprich, A. D. Daniels, O. Farkas, J. B. Foresman, J. V. Ortiz, J. Cioslowski, and D. J. Fox, Gaussian, Inc., Wallingford CT, 2009.

[S3] A. D. Becke, *J. Chem. Phys.*, 1993, **98**, 1372–1377.

[S4] C. Lee, W. Yang, R. G. Parr, *Phys. Rev. B*, 1998, **37**, 785–789.